The Astrophysical Journal, 721:738–743, 2010 September 20 doi:10.1088/0004-637X/721/1/738

THE DUAL ORIGIN OF STELLAR HALOS. II. CHEMICAL ABUNDANCES AS TRACERS OF FORMATION HISTORY

Adi Zolotov[1], Beth Willman[2], Alyson M. Brooks[3], Fabio Governato[4], David W. Hogg[1], Sijing Shen[5], and James Wadsley[5]
[1] Center for Cosmology and Particle Physics, Department of Physics, New York University, 4 Washington Place, New York, NY 10003, USA; az481@nyu.edu
[2] Haverford College, Department of Astronomy, 370 Lancaster Avenue, Haverford, PA 19041, USA; bwillman@haverford.edu
[3] California Institute of Technology, M/C 350-17, Pasadena, CA 91125, USA
[4] Department of Astronomy, University of Washington, P.O. Box 351580, Seattle, WA 98195, USA
[5] Department of Physics and Astronomy, McMaster University, Hamilton, Ontario L88 4M1, Canada
Received 2010 April 21; accepted 2010 August 2; published 2010 September 1

ABSTRACT

Fully cosmological, high-resolution *N*-body+smooth particle hydrodynamic simulations are used to investigate the chemical abundance trends of stars in simulated stellar halos as a function of their origin. These simulations employ a physically motivated supernova feedback recipe, as well as metal enrichment, metal cooling, and metal diffusion. As presented in an earlier paper, the simulated galaxies in this study are surrounded by stellar halos whose inner regions contain both stars accreted from satellite galaxies and stars formed in situ in the central regions of the main galaxies and later displaced by mergers into their inner halos. The abundance patterns ([Fe/H] and [O/Fe]) of halo stars located within 10 kpc of a solar-like observer are analyzed. We find that for galaxies which have not experienced a recent major merger, in situ stars at the high [Fe/H] end of the metallicity distribution function are more [α/Fe]-rich than accreted stars at similar [Fe/H]. This dichotomy in the [O/Fe] of halo stars at a given [Fe/H] results from the different potential wells within which in situ and accreted halo stars form. These results qualitatively match recent observations of local Milky Way halo stars. It may thus be possible for observers to uncover the relative contribution of different physical processes to the formation of stellar halos by observing such trends in the halo populations of the Milky Way and other local L* galaxies.

Key words: Galaxy: abundances – Galaxy: formation – Galaxy: halo – methods: numerical

Online-only material: color figures

1. INTRODUCTION

Observational evidence has been mounting that the stellar halo of the Milky Way (MW) was likely assembled through a combination of both hierarchical accretions and in situ star formation. The properties of local halo stars suggest that the Galaxy's halo is composed of at least two distinct but overlapping stellar populations (Carollo et al. 2010). These two halo components exhibit different spatial distributions, orbits, and metallicities, most likely because each formed through a different mechanism and on a different timescale. While the outer halo component, which dominates at distances greater than ∼20 kpc, with [Fe/H] ∼ − 2.5, is consistent with having been accreted from merged dwarf galaxies, the stars in the more metal-rich ([Fe/H] ∼ − 1.5) inner halo likely formed predominantly in situ (Norris 1994; Chiba & Beers 2000; Carollo et al. 2007, 2010).

Studies of the detailed chemical abundances of MW halo stars have sought to place further constraints on the formation of the Galactic halo (Nissen & Schuster 1997; Stephens & Boesgaard 2002; Venn et al. 2004; Pritzl et al. 2005; Ishigaki et al. 2010). These works rely on the behavior of the [α/Fe] ratio to indicate the timescale of the star formation history of the halo. Alpha elements are primarily produced in core-collapse supernovae (SNe), which occur after ∼10^7 years, while the majority of iron is produced in SNe Type Ia, whose timescale of $\leqslant 10^9$ years is significantly longer (Maoz & Badenes 2010). In the metallicity range of $-2 <$ [Fe/H] < -0.5, inner halo stars are ∼0.1 dex more alpha-rich than outer halo stars, implying that the Galaxy's halo was not uniformly enriched by core-collapse SNe (Ishigaki et al. 2010). In a local sample of stars, those with [α/Fe] ∼0.3 show a constant [α/Fe] over the above metallicity range, while stars with lower α ratio, of about 0.15, exhibit a decrease in [α/Fe] toward higher metallicity (Nissen & Schuster 2010). Similar declines to lower [α/Fe] have been observed in dwarf galaxies, though at lower [Fe/H] values (Tolstoy et al. 2009). These trends strengthen the argument that the MW's halo likely hosts two populations of stars, with distinct formation origins.

In the past year, theoretical results from galaxy simulations have been used to investigate the contribution of in situ stars to the formation history of stellar halos. Using fully cosmological *N*-body + smooth particle hydrodynamic (SPH) simulations of four stellar halos surrounding disk galaxies, Zolotov et al. (2009, hereafter Paper I) showed that while the formation of most stellar halos is dominated by accretion events, a population of in situ stars resides in the inner regions of halos as well. These in situ halo stars form in the inner most regions of the simulated galaxy and are displaced into the stellar halo through major mergers. In situ stars may also end up in stellar halos, along side accreted stars, through minor accretion events, which heat up disks and eject a small fraction of their stars into kinematic halo orbits (Purcell et al. 2010).

Previous work on the chemical abundance trends of stellar halos has relied on simulations that only allowed for the formation of stellar halos via hierarchical buildup, using dark-matter-only simulations, combined with semi-analytic models (Bullock & Johnston 2005; Robertson et al. 2005; Font et al. 2006a, 2006b; Johnston et al. 2008; De Lucia & Helmi 2008). These simulations, however, do not have the capability to examine possible chemical abundance trends for in situ halo stars.

In this paper, we use four high-resolution cosmological SPH+*N*-body simulations of disk galaxies to investigate the chemical abundance trends of both accreted and in situ halo

Table 1
Properties of Simulated Galaxies

Run	$M_{\rm vir}$ ($M_\odot$)	$N_{\rm tot}$ at $z = 0$ dark+gas+stars	$M^{\rm DM}_{\rm particle}$ ($M_\odot$)	$M^{*}_{\rm particle}$ ($M_\odot$)	$\epsilon^{\rm a}$ (kpc)	Radial Scale Length (kpc)
MW1	1.1×10^{12}	4.9×10^{6}	7.6×10^{5}	2.7×10^{4}	0.3	2.0
h277	7.4×10^{11}	2.3×10^{6}	1.2×10^{6}	4.6×10^{4}	0.35	2.6
h285	7.7×10^{11}	3.0×10^{6}	1.2×10^{6}	4.6×10^{4}	0.35	2.9
h258	7.2×10^{11}	2.5×10^{6}	1.2×10^{6}	4.6×10^{4}	0.35	4.0

Note. [a] Gravitational spline softening length.

stars. While past numerical work on chemical abundance trends in halo stars have focused solely on accreted stars, the goal of this work is to test whether in situ and accreted stars are distinguishable using chemical abundance patterns.

2. SIMULATIONS

The four high-resolution disk galaxy simulations used in this study were chosen to have approximately the same total mass, though with varied merging histories. Three of these simulations (MW1, h277, and h285) are discussed in detail in Paper I and references therein, while the remaining simulation (h258) is described in Governato et al. (2009). These disk-dominated galaxies were simulated using GASOLINE (Wadsley et al. 2004). We briefly summarize the important features of these simulations below. MW1 has a total mass of $10^{12}\ M_\odot$, while the remaining three galaxies, h277, h258, and h285, all have a total mass of $\sim 7.6 \times 10^{11}\ M_\odot$. All have several million particles (dark matter + gas + stars) within their virial radius at $z = 0$. Table 1 lists the primary properties of all four simulations. A physically motivated recipe was used to describe star formation and SN feedback (Stinson et al. 2006; Governato et al. 2007) with a uniform UV background that turns on at $z = 9$, resembling cosmic reionization (Haardt & Madau 1996).

Because this work aims to examine the metallicity and alpha abundances of halo stars, the details of the treatment of chemical enrichment are important to this paper. All of the galaxies used in this study have been rerun since Paper I with metal cooling and metal diffusion, which realistically captures the effect of the turbulent interstellar medium (ISM) on metal mixing (Shen et al. 2010). Metal cooling increases the amount of star formation in these galaxies, and therefore the amount of energy deposited into the local ISM by SN has been increased from 0.4, in Paper I, to 0.7×10^{51} erg. The SN feedback employed in these simulations deposits the energy into the ISM and cooling is turned off for a period of time for those gas particles within the SN blast wave radius. As described in detail in Stinson et al. (2006), SN Type Ia and II yields are adopted from Thielemann et al. (1986) and Woosley & Weaver (1995), respectively, and implemented following Raiteri et al. (1996). We follow oxygen and iron yields from SNe Type Ia and core-collapse SNe, and use [O/Fe] as our proxy for [α/Fe]. These galaxies follow observed local metallicity trends (Brooks et al. 2007), as well as metallicity trends at high redshift (Maiolino et al. 2008; Pontzen et al. 2008, 2010).

2.1. Selecting "Observed" Halo Stars

Each simulated galaxy used in this study has been decomposed into a disk, bulge, and halo kinematic component, using the full six-dimensional phase-space information available for all stars. We use the same decomposition technique as in Paper I, but provide all the relevant details here. In order to decompose the disk from the spheroid, we first align the angular momentum vector of the disk with the z-axis. This places the disk in the x–y plane and allows us to calculate the angular momentum of each star in that plane, J_z, as well as the momentum of the co-rotating circular orbit with similar orbital energy, $J_{\rm circ}$. A star with a circular orbit in the plane of the disk will have $J_z/J_{\rm circ} \sim 1$ in this framework. Stars with $J_z/J_{\rm circ} \geqslant 0.8$ are selected as disk stars. This cut is equivalent to an eccentricity cut of $e \leqslant 0.2$, which matches the eccentricities observed in the MW's disk (Nordström et al. 2004).

In this study, we use only those stars which have orbital characteristics of a stellar halo population. The spheroid (halo + bulge) of each galaxy is defined using a cut in $J_z/J_{\rm circ}$ such that the spheroidal population does not exhibit a net rotation. We can further decompose the spheroid into a bulge and halo because a break in the mass density profile is observed. Stars which are tightly bound to the galaxy—those whose total energy is low—are classified as bulge stars, while all other stars are identified as halo stars. The energy cut employed is set in order to make a two-component fit to the mass profile of the spheroid. Bulge stars are within the break of the mass profile, and halo stars are outside the break. Although there are stars whose kinematics do not make either the disk or the spheroid cuts (thick disk and pseudo bulge stars), they are not relevant to this study. Only stars which have been identified by this procedure as belonging to the kinematic halo population are used in this study.

After we have selected the kinematic halo population using the above procedure, we go on to create an observational sample similar to the sample of halo stars in Sloan Digital Sky Survey (SDSS) used by Carollo et al. (2010). To simulate an observer at the solar position, we place the "Sun" at a distance of $\sim$3 disk radial scale lengths away from the center, and then calculate the heliocentric distances of each star. The radial scale length of each simulated disk is listed in Table 1. While Carollo et al. (2010) only observe stars out to a volume less than 4 kpc from the Sun, we have chosen to study halo stars within 10 kpc of the simulated heliocentric observer. The foremost reason for this 10 kpc cutoff is that nearly all of the in situ stars ($\geqslant$80%, described in the following section) in the simulated halos are within the inner $\sim$10 kpc of the stellar halos. Second, many studies of the MW's stellar halo have used F- and G-type stars, which are currently observed out to a few tens kiloparsecs. To match a large ground-based survey like SDSS, we restrict our observed sample to stars more than 30° above and more than 1 kpc above the plane of the disk, for a heliocentric observer.

Stars that are classified as belonging to the halo in the kinematic decomposition and which fit the spatial and SDSS-like cuts are referred to as part of the observed halo sample. Table 2 lists the total stellar mass in each galaxy's halo, as well as the fraction of in situ and accreted stars in each observed halo sample.

Table 2
Stellar Halo Origins

Run	Total Halo Mass ($M_\odot$)	Accreted Fraction (% in Obs. Sample)	In situ Fraction (% in Obs. Sample)	Ambiguous Fraction[a] (% in Obs. Sample)	$z_{1\,\mathrm{mm}}$[b]
MW1	6.9×10^9	65	31	4	3
H277	9.22×10^9	72	25	3	3
H285	2.7×10^{10}	91	6	3	2
H258	1.59×10^{10}	87	10	3	1

Notes. The total mass listed for each halo is the total halo stellar mass within the virial radius. The accreted, in situ, and ambiguous fractions are for the stars within each observed halo sample, as described in Section 2.1.

[a] The origin of these stars is ambiguous due to the finite time resolution of the simulation, as described in Section 2.2.

[b] The redshift of the last significant major merger, defined as a merger with mass ratio $\frac{M_{\mathrm{primary}}}{M_{\mathrm{secondary}}} < 7$.

2.2. Halo Star Origin—Accreted Versus In Situ

We trace the formation history of each star particle located within the virial radius of the main galaxy at $z = 0$ back to $z = 6$, as well as follow the gas particles from which the stars have formed. At each time step output by the simulation (every 25 Myr), we identify the dark-matter halo to which each particle belonged using AHF[6] (Gill et al. 2004; Knollmann & Knebe 2009). A star is considered bound to a dark-matter halo only if it is identified as belonging to that halo for at least two consecutive time steps. Using this technique, we identify three different formation origins: accreted, in situ, and ambiguous. For a detailed description of this procedure and a discussion of numerical issues, the reader is referred to Paper I. We quickly review the three classifications below.

Accreted stars formed in halos other than the main galaxy's dark-matter halo. Through merging, these stars have become unbound to their progenitors and now belong to the main galaxy's halo. The majority of the accreted stars in the halos of h277, h285, and MW1 (75% by mass in stars) originated in two to three subhalos, each with a total mass of 1–3 $\times 10^{10}\ M_\odot$. The majority of accreted stars in h258, which experiences several major mergers, as discussed in Section 3, originate in three galaxies, with total masses ranging from 2.5 to 6 $\times 10^{10}\ M_\odot$.

In situ stars, on the other hand, formed within the main galaxy's potential well, with their gas progenitors bound to the main galaxy before their formation. Paper I found this population formed within the inner ~4 kpc of the galaxy's center before being displaced into the kinematic halo component as a result of mergers. Stars which are classified as ambiguous, ~3% of the total halo stars, have an unknown formation history due to the limited number of time steps output for each simulation. This occurs if a gas particle spawns a star particle at approximately the same time that it first becomes bound to the primary. In such cases, it is uncertain whether the star formed in the primary or in its original subhalo.

All four of the simulated galaxies analyzed in this paper host a stellar halo which contains both accreted and in situ stars. While the relative contribution of each population differs from halo to halo, the presence of stars with a dual origin is a generic feature of the stellar halos surrounding L* galaxies at $z = 0$. In Paper I, we showed that the fraction of in situ stars present in a halo strongly depends on the merging history of the primary galaxy. Galaxies with active merging histories host massive accreted halos, resulting in a small fractional contribution from the in situ halo population. Conversely, in galaxies which have not accreted as many stars during their lifetimes, the in situ population is less diluted and contributes more to the total halo mass. As suggested by their in situ fractions, h285 and h258 have much more active merging histories than MW1 and h277 (Table 2).

3. TRENDS IN CHEMICAL ABUNDANCES WITH FORMATION ORIGIN

We now examine the trends in chemical abundances displayed by the observed halo stars. One expects that the chemical abundance pattern of a stellar population will be set by the star formation history of the galaxy in which the population formed. For this reason, we aim to find trends which differentiate the in situ and accreted populations in each stellar halo. These qualitative trends in metallicity are robust and applicable not just to the MW, but to MW-mass galaxies with different merging histories, as discussed in detail below and in Section 4.

Massive galaxies form in deep potential wells and consequently have higher star formation rates (SFRs) than less-massive galaxies, resulting in a mass–metallicity relation (Tremonti et al. 2004; Brooks et al. 2007; Finlator & Davé 2008). With their high SFR, massive galaxies will reach higher [Fe/H] at relatively constant [α/Fe] before SNe Ia begin to contribute, as core-collapse SNe enrich the ISM with mostly alpha elements, and little iron or iron-peak elements. In lower mass galaxies, however, lower SFRs mean that the galaxy cannot enrich as much in Fe before SNe Type Ia began to contribute, resulting in a decrease of [α/Fe] at lower [Fe/H]. Additionally, galaxies with long star formation histories will form stars out of gas that has been enriched by both core-collapse SNe and SNe Type Ia, whereas galaxies with truncated star formation histories will have their abundance pattern set primarily by core-collapse SNe. These trends are shown in Figure 1.

If the in situ and accreted populations each formed at different times, under different physical conditions, we expect to see that reflected in their abundance patterns. We indeed find that in three of our galaxies (those without a very recent major merger) in situ halo stars at the high [Fe/H] end of the metallicity distribution function (MDF) tend to be more alpha-rich than the similarly high [Fe/H] accreted stars (Figure 3, discussed in detail below). At lower [Fe/H], we find that the two populations have similar [O/Fe]. Because we only follow oxygen and iron in these simulations, [O/Fe] serves as our proxy for [α/Fe].

Before we discuss our findings in detail, it is important to first note that the satellites of the simulated galaxies studied here are brighter, and hence are more [Fe/H]-rich, than those observed in the MW (Zolotov et al. 2009). If the satellites which built up our simulated stellar halos contained less stellar mass at a given total mass, the qualitative chemical abundance patterns for in situ and accreted halo stars discussed below would not change, as we demonstrate in detail in Section 4. The results in

[6] AMIGA's HALO FINDER, available for download at http://popia.ft.uam.es/AMIGA.

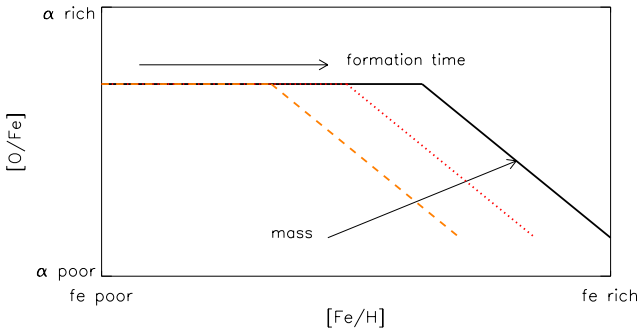

Figure 1. Evolution of [Fe/H] vs. [α/Fe] (tracked by [O/Fe] in our simulations) as a function of a stellar population's formation time and the mass of the galaxy in which they form. The black solid line represents the most massive galaxy, the red dotted line an intermediate mass galaxy, and the orange dashed line a low-mass galaxy. Higher mass galaxies have higher SFRs, and therefore enrich with more core-collapse SN in a given time, reaching a higher [Fe/H] before turning over to lower [α/Fe] compared to a low-mass galaxy with a slower SFR in the same amount of time.

(A color version of this figure is available in the online journal.)

metallicity we discuss, however, are not meant to be absolute, and the qualitative trends are robust for MW-mass galaxies.

As discussed in Section 2.2, in situ stars formed in the innermost regions of the primary galaxy's dark-matter halo and were displaced into the halo through massive mergers. Since the redshift of the last significant merger (Table 2) determines the last time at which in situ stars are substantially displaced into the halo, the formation time of the in situ populations of each galaxy is quite different. The left panel of Figure 2 shows the time of formation for in situ halo stars (solid lines) and accreted halo stars (dashed lines) in each simulated observed sample. Because MW1 and h277 experience their last significant merger early on, at $z \sim 3$, the in situ stars in these galaxies all formed before $t < 2.5$ Gyr. The late mergers of h285 and h258, at $z = 2$ and $z = 1$, respectively, result in younger in situ populations in these halos. The right panel of Figure 2 shows the time at which accreted halo stars first became unbound from their satellites and were accreted onto the primary halo. While the majority of the accreted stars in h277 and MW1 become bound to these galaxies early on (with 90% of such stars being accreted at times $\leqslant$4 Gyr), h285 and h258 accreted a large number of their halo stars at times later than this.

Figure 3 shows [Fe/H] versus [O/Fe] of in situ halo stars (in red triangles) and accreted halo stars (in black circles) for each simulated observed halo sample. We find that in MW1 and h277 (two top panels of Figure 3), where 80% of in situ halo stars formed within a 1 Gyr time span in a deep potential well, the ISM did not have time to enrich with SNe Type Ia, and so the [α/Fe] of these stars is approximately constant with [Fe/H]. The accreted stars in these halos, however, formed slightly later on and in shallower potential wells than the in situ stars. They thus experienced a lower SFR, resulting in a decrease of their [α/Fe].

While the accreted stars of h285 (bottom left panel of Figure 3) display a similar trend in [α/Fe] to the accreted populations of h277 and MW1, its in situ population does not display a constant [α/Fe] like the other galaxies. The in situ population of this galaxy had more time to form (because of the later merger) and formed in a smaller galaxy than MW1 and h277's in situ stars. At $z = 3$, the total virial masses of h277 and MW1 are $8.5 \times 10^{10}\,M_{\odot}$ and $1 \times 10^{11}\,M_{\odot}$, respectively, whereas h285's mass is only $5 \times 10^{10} M_{\odot}$. Because of this, the in situ stars of h285 display a turnover in [O/Fe] at lower [Fe/H], rather than remaining constant at higher metallicities like MW1 and h277.

Unlike the other galaxies, h258 (bottom right panel of Figure 3) experiences a nearly 1:1 merger at $z = 1$. The in situ and accreted stars in this galaxy do not follow a similar trend to the other galaxies. The in situ halo population in this galaxy had more time to form (Figure 2, left panel), and hence were enriched to a lower [α/Fe] than the other in situ halo populations. Furthermore, because of its binary merger, many of the h258 in situ stars have similar chemical abundances to the accreted population. This galaxy has undergone three massive accretion events in its lifetime, whose "tracks" are evident in Figure 3.

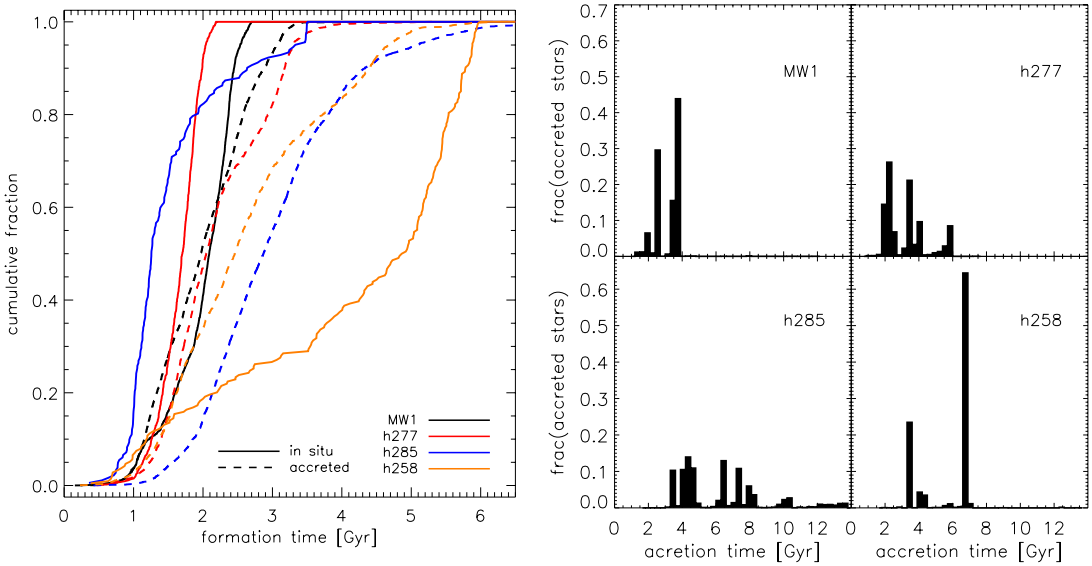

Figure 2. Left panel: Fractional contribution of accreted and in situ stars to each of the four simulated observed halo samples, as a function of the populations' formation time. In situ stars are shown in solid lines, while accreted stars are shown in dashed lines. Right panel: Accretion history of each simulated observed halo sample. The accretion time shown is the time at which each star became unbound from its progenitor and was accreted onto the primary halo. Both h285 and h258 have a higher contribution from late accretion events than MW1 and h277.

(A color version of this figure is available in the online journal.)

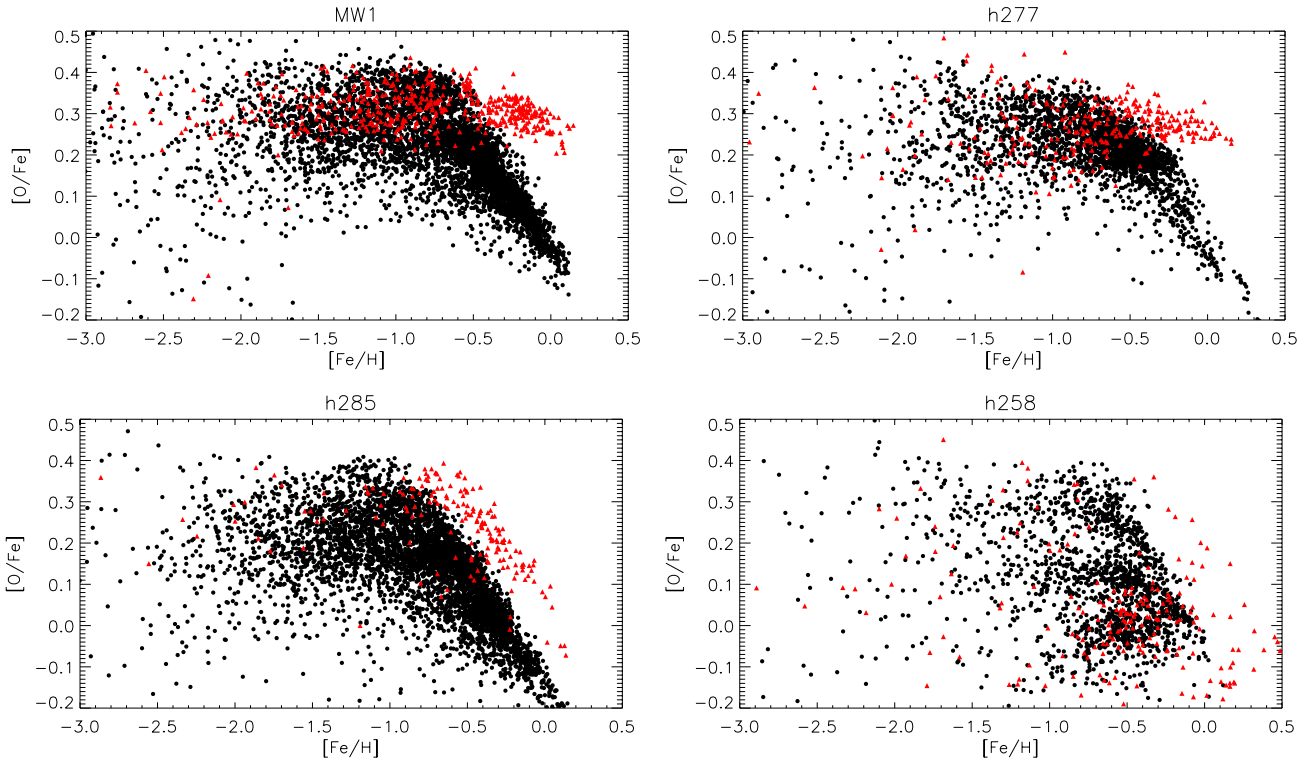

Figure 3. [O/Fe] vs. [Fe/H] for observed halo stars in each of the four simulated galaxies studied in this paper. In situ stars are shown in red triangles, and accreted stars in black dots. Accreted stars dominate the stellar halos of all the galaxies studied here. The in situ stars of MW1, h277, and h285, which formed relatively early on in the center of these galaxies, are more alpha-rich at high metallicity than accreted stars. The same is not true for h258 (shown in the bottom right panel), as discussed in Section 3. The satellites of the galaxies studied here are overluminous and so halo stars are more metal-rich in this study than expected from observations, as discussed in detail in Section 4.

(A color version of this figure is available in the online journal.)

4. SIMULATION EFFECTS

The primary result of this study is that in situ halo stars have higher [α/Fe] than accreted halo stars at the high [Fe/H] end of the MDF. In this section, we discuss the role of simulation effects in this study and the robustness of our primary results to these effects.

The most relevant numerical issue in this study is that the satellites of the simulated galaxies are brighter than those observed in the MW (Zolotov et al. 2009). While the MW hosts only two satellites with $-19 < M_v < -16$, the Large and Small Magellanic Clouds, the four simulated galaxy halos have, on average, four satellite companions in this luminosity range at $z = 0$. Brighter satellites will of course contribute more accreted stars to a given stellar halo. This affects our results in two pertinent ways. First, the fractional contribution of in situ stars to each stellar halo is likely underestimated, as discussed in Paper I. Second, because our simulated satellites contain too many stars, they are also more [Fe/H]-rich than we expect for the satellites that contributed to MW-mass stellar halos.

The differing [α/Fe] trends displayed by the in situ and accreted halo components are a robust prediction for MW-massed galaxy halos that are not undermined by the details of the present simulations' MDFs. Had our simulated halos been built up from satellites that were less luminous at a given total satellite mass, the trends shown in Figure 3 would have simply been shifted to lower [Fe/H]. To demonstrate this, we have re-simulated one of the galaxies in this paper (MW1) with the same exact initial conditions but with differently calibrated SN feedback and star formation. The physical treatment of these processes is unchanged in the new simulation. The new run employed a stronger SN feedback, with an increase in thermal SNe energy from 0.7 to 1 $\times 10^{51}$ erg, and the threshold for star formation density has been increased from 0.1 to 1 amu cm^{-3}. As a result of the stronger feedback and higher density threshold, at $z = 0$, the new simulated halo hosts only two satellites in the luminosity range $-19 < M_v < -16$. The new MW1 stellar halo also has an MDF that is similar to that observed of halo stars in M31 (Kalirai et al. 2006). In the inner 30 kpc of its stellar halo, stars in the new MW1 have $< [\mathrm{Fe/H}] >\sim -0.9$.

Figure 4 shows [O/Fe] versus [Fe/H] for a $z = 2$ satellite for the new run with stronger feedback (top panel) and for the MW1 used in this paper (bottom panel). We have chosen to look at $z = 2$ satellites because 95% of accreted stars which end up in our halo sample (see Figure 2) formed before this time in such satellites. The total mass of both satellites is $\sim 9.4 \times 10^9\ M_\odot$, but the stellar mass of the new satellite is 4.5×10^8 and that of the old satellite is $1.5 \times 10^9\ M_\odot$. Both satellites exhibit the characteristic turn over to lower [O/Fe]. The new run with the less-luminous satellite population simply exhibits this turn over at a lower [Fe/H]. The in situ stars of each galaxy are shown in red triangles. Both simulations show that in situ stars are more alpha-rich at the high [Fe/H] end than the satellite stars. The distinct [α/Fe] trends of the two halo populations are a result of their formation in potential wells whose depths vary by more than an order of magnitude. The trends do not depend on the details of the simulations' MDF.

5. DISCUSSION AND CONCLUSIONS

In this paper, we have studied the chemical abundance trends of inner halo stars in four SPH+*N*-body simulations of

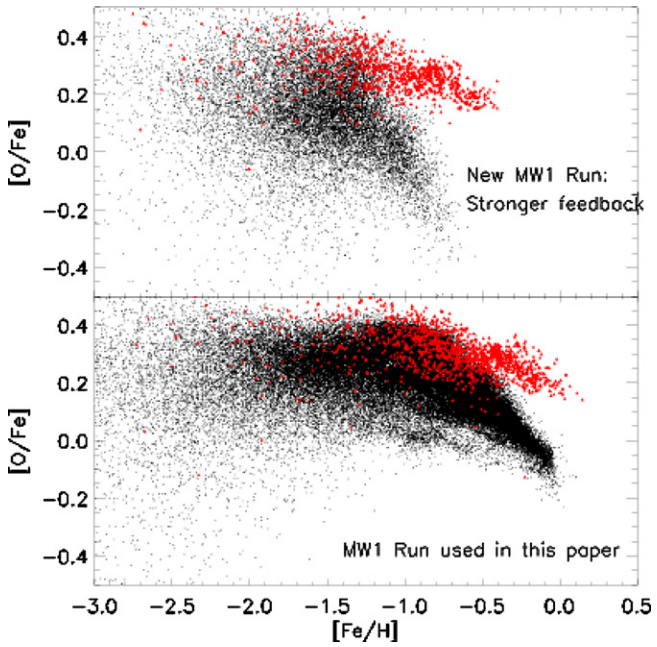

Figure 4. [O/Fe] vs. [Fe/H] for $z = 2$ satellite stars (shown in black) in one of the simulations discussed in this paper (bottom panel) and in a satellite of a new simulation, with identical initial conditions, but a stronger SNe feedback (top panel). In situ stars are shown in red triangles. See Section 4 for details. Such satellites are typical contributors to the $z = 0$ accreted populations in our halos. Employing a stronger SNe feedback in the simulations results in more metal-poor stars, though both runs display the same qualitative trend that the in situ stars are more alpha-rich than the accreted stars at the high-metallicity end.

(A color version of this figure is available in the online journal.)

approximately L* disk galaxies. We investigate the possibility of using chemical abundance trends to discern the relative importance of in situ and accretion processes in building up the inner stellar halos of MW-mass galaxies. For each simulated galaxy, we concentrated on a sample of halo stars located within 10 kpc of a simulated Sun-like observer. This sample included stars from two populations, one formed in situ and the other accreted. We find that in the inner halos of galaxies where a recent binary merger did not occur, high [Fe/H] in situ halo stars are more [α/Fe]-rich than accreted stars at similar [Fe/H].

The bimodal distribution of [α/Fe] at high [Fe/H] for in situ and accreted stars is primarily due to the different mass galaxies in which they formed. The in situ halo populations (in all but h258) were formed early on deep in the potential wells of the primary dark-matter halos, where a high SFR ensured that only core-collapse SNe dominated the chemical enrichment up to high [Fe/H]. The accreted stars, which formed later, on average, than the in situ stars and in shallower potential wells, underwent a slower chemical evolution, where SNe Type Ia contributed iron at lower [Fe/H], resulting in a lower [α/Fe] at a given [Fe/H]. Such trends are expected given a mass–metallicity relation (Brooks et al. 2007). Though the satellite galaxies in our simulations are too bright and hence too metal-rich, we have found that the relative chemical abundance patterns between in situ and accreted stars is a qualitative trend that is robust to the details of the simulated halos' MDFs.

We predict that a large systematic survey of the detailed chemical abundances of inner halo stars in the MW will exhibit such dual trends in [Fe/H] versus [α/Fe]. At higher metallicities, [Fe/H] $\geqslant -1.0$, MW stars in the inner several kiloparsecs of the halo should exhibit a bimodal distribution in [α/Fe]. Unless the Galaxy has experienced a recent major merger, high [α/Fe] stars in this metallicity range will have formed in the MW's disk or bulge and then been displaced into halo orbits. Low [α/Fe] stars in this regime will likely have formed in smaller potential wells than the MW and were accreted from satellite companions at high redshift. In fact, such trends in α and Fe have already been observed in a small sample of 94 local MW halo dwarfs (Nissen & Schuster 2010). Larger planned surveys, like HERMES, which will obtain high-resolution spectra of MW halo stars will be able to observe such patterns and quantify the importance of different physical processes to the MW's halo formation.

We thank the anonymous referee for helping to greatly improve the paper. We thank Chris Brook for helpful conversations and Joe Cammisa at Haverford for computing support. A.Z. and B.W. acknowledge support from the NSF grant AST-0908446. All simulations were run using the NASA Advanced Supercomputer Pleiades. F.G. acknowledges support from the HST GO-1125, NSF AST-0607819, and NASA ATP NNX08AG84G grants. A.M.B. acknowledges support from the Sherman Fairchild Foundation.

REFERENCES

Brooks, A. M., Governato, F., Booth, C. M., Willman, B., Gardner, J. P., Wadsley, J., Stinson, G., & Quinn, T. 2007, ApJ, 655, L17
Bullock, J. S., & Johnston, K. V. 2005, ApJ, 635, 931
Carollo, D., et al. 2007, Nature, 450, 1020
Carollo, D., et al. 2010, ApJ, 712, 692
Chiba, M., & Beers, T. C. 2000, AJ, 119, 2843
De Lucia, G., & Helmi, A. 2008, MNRAS, 391, 14
Finlator, K., & Davé, R. 2008, MNRAS, 385, 2181
Font, A. S., Johnston, K. V., Bullock, J. S., & Robertson, B. E. 2006a, ApJ, 638, 585
Font, A. S., Johnston, K. V., Bullock, J. S., & Robertson, B. E. 2006b, ApJ, 646, 886
Gill, S. P. D., Knebe, A., & Gibson, B. K. 2004, MNRAS, 351, 399
Governato, F., Willman, B., Mayer, L., Brooks, A., Stinson, G., Valenzuela, O., Wadsley, J., & Quinn, T. 2007, MNRAS, 374, 1479
Governato, F., et al. 2009, MNRAS, 398, 312
Haardt, F., & Madau, P. 1996, ApJ, 461, 20
Ishigaki, M., Chiba, M., & Aoki, W. 2010, PASJ, 62, 143
Johnston, K. V., Bullock, J. S., Sharma, S., Font, A., Robertson, B. E., & Leitner, S. N. 2008, ApJ, 689, 936
Kalirai, J. S., et al. 2006, ApJ, 648, 389
Knollmann, S. R., & Knebe, A. 2009, ApJS, 182, 608
Maiolino, R., et al. 2008, A&A, 488, 463
Maoz, D., & Badenes, C. 2010, MNRAS, in press
Nissen, P. E., & Schuster, W. J. 1997, A&A, 326, 751
Nissen, P. E., & Schuster, W. J. 2010, A&A, in press (arXiv:1002.4514)
Nordström, B., et al. 2004, A&A, 418, 989
Norris, J. E. 1994, ApJ, 431, 645
Pontzen, A., et al. 2008, MNRAS, 390, 1349
Pontzen, A., et al. 2010, MNRAS, 402, 1523
Pritzl, B. J., Venn, K. A., & Irwin, M. 2005, AJ, 130, 2140
Purcell, C. W., Bullock, J. S., & Kazantzidis, S. 2010, MNRAS, 404, 1711
Raiteri, C. M., Villata, M., & Navarro, J. F. 1996, A&A, 315, 105
Robertson, B., Bullock, J. S., Font, A. S., Johnston, K. V., & Hernquist, L. 2005, ApJ, 632, 872
Shen, S., Wadsley, J., & Stinson, G. 2010, MNRAS, in press
Stephens, A., & Boesgaard, A. M. 2002, AJ, 123, 1647
Stinson, G., Seth, A., Katz, N., Wadsley, J., Governato, F., & Quinn, T. 2006, MNRAS, 373, 1074
Thielemann, F., Nomoto, K., & Yokoi, K. 1986, A&A, 158, 17
Tolstoy, E., Hill, V., & Tosi, M. 2009, ARA&A, 47, 371
Tremonti, C. A., et al. 2004, ApJ, 613, 898
Venn, K. A., Irwin, M., Shetrone, M. D., Tout, C. A., Hill, V., & Tolstoy, E. 2004, AJ, 128, 1177
Wadsley, J. W., Stadel, J., & Quinn, T. 2004, New Astron., 9, 137
Woosley, S. E., & Weaver, T. A. 1995, ApJS, 101, 181
Zolotov, A., Willman, B., Brooks, A. M., Governato, F., Brook, C. B., Hogg, D. W., Quinn, T., & Stinson, G. 2009, ApJ, 702, 1058